Article ID: 1000-324X(2015)04-0443-06 **DOI:** 10.15541/jim20140526

Ultra-long VO_2(B) Nanobelts : One-step Hydrothermal Synthesis and Electrochemical Properties

YANG Xue -Mei[1, 2], LIU Zhong -Ping[1, 2], LI Xiao -Dong[1, 2], Zhang Ze -Ming[2], JI Lan-Xiang[2], DENG Jian-Guo[1, 2]

(1. Institute of Chemical Materials, China Academy of Engineering Physics, Mianyang 621900, China; 2. Sichuan Research Center of New Materials, Mianyang 621000, China)

Abstract: Ultra-long VO_2(B) nanobelts were fabricated by a facile one-step hydrothermal treatment. It was found that the nanobelts were about ~200 nm in width and dozens of microns in length. Being used as a cathode material, the VO_2(B) nanobelts show superior rate capability, with discharge capacities of *ca.* 425, 175, 125, 90, 75 and 50 mAh/g at 50, 100, 200, 500, 1000 and 2000 mA/g, respectively. More importantly, excellent cycling stability without considerable capacity loss (10.41%) for 500 cycles is observed. The present study implied that the unique ultra-long nanobelts morphology and its intrinsic structural features are responsible for their excellent structure stability, and thus resulting in superior electrochemical performance.

Key words: VO_2(B); nanobelt; electrochemical property

The storage of energy through electrochemical reactions is a crucial technology for portable power needs[1-6]. Due to layered structures and promising properties in nanometer region, nanostructured VO_2(B) materials have been widely studied and considered good alternatives to the carbon-based canode materials in Li-ion batteries (LIBs) and supercapaciters (SCPs)[7]. Recently, Tarascon, *et al* gaves an amazement that crystalline VO_2(B), synthesized *via* a low temperature heat treatment in vacuum, exhibited a specific capacity as high as 500 mAh/g[8]. Hierarchical VO_2(B) nanoparticles prepared by electrospinning shown an initial and 50th discharge capacities of up to 390 and 201 mAh/g, respectively[9]. All of these studies have successes, however, their structures could hardly display a long-term stable cycling performance.

On the other hand, it should be noted that the performance depends not only on the structure, but also on the morphology of the electrode components[10-13]. One-dimensional nanomaterials with large length to diameter ratio and good electronic transport properties has a broad application prospect in electrochemical energy storage, electronics and other fields[14]. With regard to vanadium oxide, various materials with 1D nanostructures, such as VO_2(B) nanobelts, V_3O_7 nanofibers, V_2O_5 nanobelts, *etc*., have been synthesized and obtained improved electrochemical properties extensively[15-20].

In this study, we report a facile one-step hydrothermal method to directly synthesize ultra-long VO_2(B) nanobelts, and the optimal synthesis condition in detail.

1 Experimental procedure

1.1 Synthesis

All the starting materials, V_2O_5 and butylated hydroxytoluene (BHT) were analytically pure and used without purification. In a typical procedure, 2.5 mmol (0.4547 g) V_2O_5 and 5 mmol (1.1018 g) BHT were stirred with 80 mL deionized water. After stirring for about 2 h, the obtained yellow solution was transferred to a 100 mL Teflon-lined stainless steel autoclave followed by hydrothermal treatment at 20℃ for 24 h. After the autoclave was cooled to room temperature, the resultant blue-black products were washed with firstly deionised water and ethanol. Finally, the ultra-long VO_2(B) nanobelts powers were obtained after drying at 60℃ for 5 h.

1.2 Characterization

The phase structure were determined by powder X-ray diffraction (XRD) using Cu Kα radiation (λ= 0.15418 nm). The morphologies were observed by scanning electron microscope (SEM) and transmission electron microscope (TEM). X-ray photoelectron spectroscope (XPS) was used to confirm the oxidation state of vanadium. The micro structural was analyzed through high-resolution TEM (HRTEM) and selected area electron diffraction (SAED).

Received date: 2014-10-20; **Modified date:** 2014-12-22; **Published online:** 2015-01-20
Biography:YANG Xue -Mei(1985–), female, candidate of Master degree. E-mail: ymmy20050410@163.com
Corresponding author: DENG Jian-Guo, professor. E-mail: jianguo_deng@caep.ac.cn; LIU Zhong-Ping, associate professor. E-mail: liuzp@caep.ac.cn

1.3 Electrochemical properties analysis

The electrochemical button cells were constructed by mixing active material, polyvinylidene fluoride (PVDF), and carbon black in the weight ratio of 80: 10: 10. Tetrahydrofuran was used as the solvent. The slurry was cast onto Al foil using a doctor-blade technique. After solvent evaporation at 70℃ and heating at 100℃ under vacuum for 12 h, the electrodes were cut into disks and assembled into CR2032 button cells with commercial electrolyte (Merck; 1 mol/L LiPF6 in 1:1 *V*/*V* ethylene carbonate : dimethyl carbonate) and Li metal counter electrode. The amount of the active material in each electrode disk is average 2.38 mg. The cells were constructed in an Ar-filled MBraun glovebox and then cycled galvanostatically at a desired current density with a Land CT2001A tester system at room temperature.

2 Results and discussion

The nanobelts were characterized by XRD pattern to identify the crystallographic structure, as shown in Fig. 1(a). All the diffraction peaks can be indexed to monoclinic structure of VO_2(B) (JCPDS 81-2392), which verifies the phase purity. The sharp diffraction peaks imply that the obtained VO_2(B) nanobelt is well crystallized. A low-magnification SEM image (Fig. 1(b)) clearly reveals that a large quantity of ultra-long (dozens of microns in length) nanobelts were achieved. The nanobelts were rather uniform with a width of ~200 nm, as confirmed from Fig. 1(c). The TEM images of VO_2(B) clearly show that the ultra-long nanobelts are randomly oriented as shown in Fig. 1(d). The interplanar distances of 0.503 nm match well with the $d_{(201)}$spacings of monoclinic VO_2(B) structure. Furthermore, according to the selected lattice planes in the SAED patterns (insets of Fig. 1(e)), all the measured interplanar distances agree well with those calculated from monoclinic VO_2(B) crystallographic parameters. These coincident spacing values provided the microscopic evidence for the existence of monoclinic VO_2(B). Moreover, the corresponding SAED image suggests that each nanobelt is in a single crystal form.

Important information on the surface composition and chemical element valence state was provided by XPS measurements, as shown in Fig. 2. Apart from C, O, and V, no other elemental peaks are shewing on the XPS spectrum (Fig. 2(a)). The C1s peaks can be attributed to the CO_2 adsorbed on the sample surfaces. The V2p core-level spectrum (Fig. 2(b)) shows peaks at 516.57 eV for V2p3/2[21] and 524.2 eV for V2p1/2[22], both the characteristic of vanadium in the +4 oxidation state which agree with the bulk VO_2 values reported in other studies.

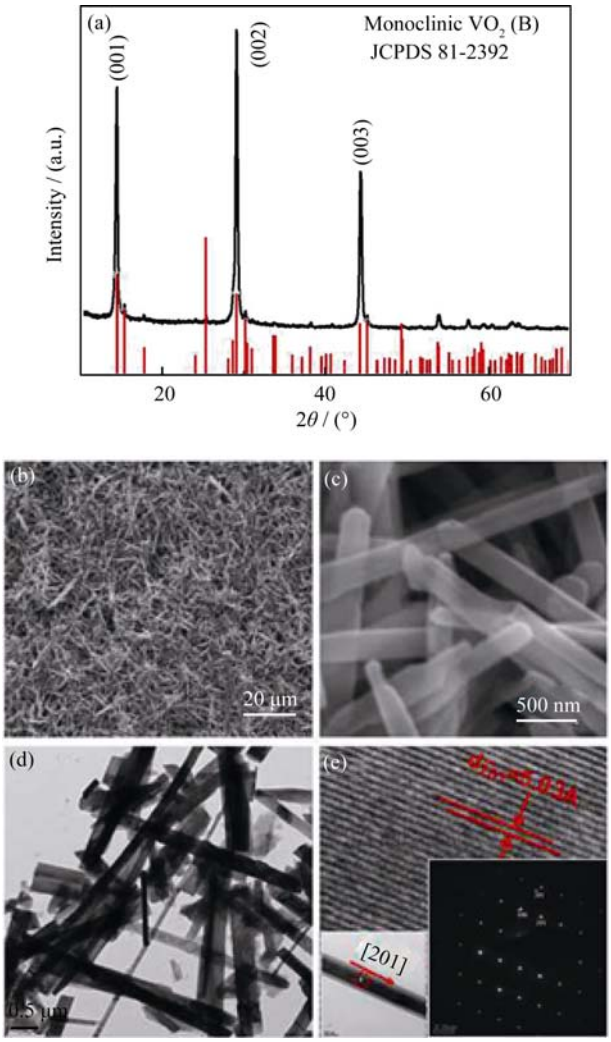

Fig. 1 Characterizations of as-prepared VO_2 nanobelts
(a) XRD patterns of VO_2(B) nanobelts; (b), (c) SEM images of VO_2(B) nanobelts; (d) low-resolution TEM images of the VO_2 (B) nanobelts and (e) HRTEM image of the end of VO_2 nanobelts showing that the nanobelt is single crystalline and free from dislocation and defects

2.1 Effects of synthesis conditions

The reaction temperature, time, and molar ratio of the reducing agent to the vanadium source (MR) are highly important for formation of ultra-long VO_2(B) nanobelts. Figure 3 shows the XRD patterns of the samples obtained at 200℃ for 24 h with different MR. Figure 3(a) shows that most of the peaks belong to V_3O_7 (H_2O) (JCPDS85-2401) when MR is 1: 1, indicating that the influence of amount of reducing agent on products is lower than others and V^{5+} cannot be adequately reduced to form V^{4+}. When MR was increased to 2: 1, the products were pure VO_2(B), [shown in Fig. 3(b)]. However, when the MR was further increased to 3: 1, the mixture of VO_2(B) and VO_2(A) were obtained. These results indicate that the MR = 2: 1 is a suitable parameter of reducing agent, under which condition V^{5+} can be adequately reduced to V^{4+} to form pure VO_2(B).

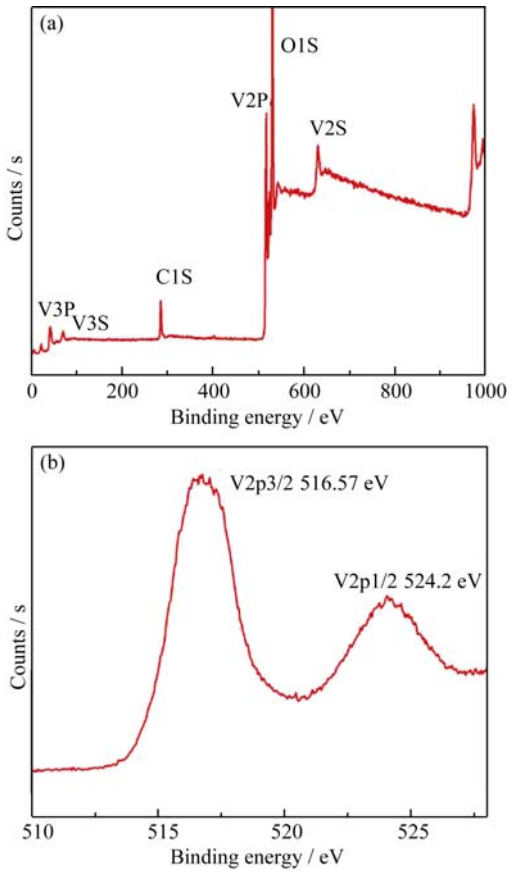

Fig. 2　(a) XPS spectrum of a typical VO_2 powder and (b) core-level spectrum of V2p

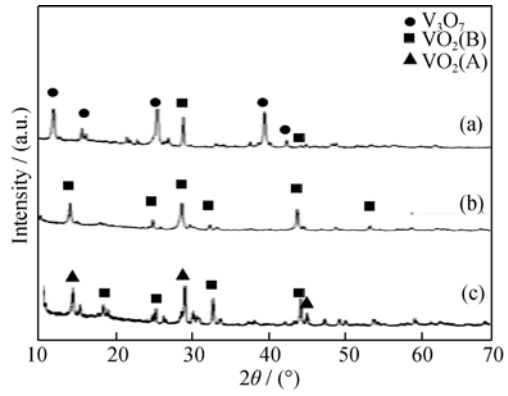

Fig. 3　XRD patterns of samples obtained with different MR
(a) MR= 1: 1; (b) MR= 2: 1; (c) MR=3: 1

Figure 4(a)-(c) reveals the effect of the reaction temperature on the phase structure under MR=2: 1. When the temperature is 180℃ and 200℃, all the peaks are consistent with VO_2(B), nevertheless, the crystallinity of VO_2(B) increases with increasing temperatures, as shown in Fig. 4(a) and (b). When temperature was increased to 220℃, the achieved products were mixture of VO_2(B) and VO_2(A), as shown in Fig. 4(c). These results reveal that high temperature leads to phase shifting from VO_2(B) to VO_2(A). On the basis of above mentioned results, we concluded that both of large amount of reducing agent and high temperature facilitate formation of VO_2(A). Consequently, a molar ratio of 3: 1 was used in the subsequent experiment as shown in Fig. 4 (d)-(f). As expected, when the temperature is 220℃, all XRD peaks can be unambiguously indexed to the standard PDF JCPDS 70-2716 of VO_2(A). Moreover, differences from the results with MR=2: 1, the VO_2(A) was observed at a lower temperature of 200℃. These results indicate that the large amount of reducing agent decrease the phase shifting temperature. In conclusion, the MR=1: 1 and low temperature lead to V_3O_7 (H_2O), the MR=3: 1 and high temperature lead to the formation of VO_2(A), and MR=2: 1 and 200 ℃ are deemed an appropriate conditions to the formation of VO_2(B), under which condition V^{5+} be adequately reduced to form V^{4+}.

The XRD patterns of the samples obtained with different reaction time (Fig. 5) reveal the evolution process of VO_2(B). From the XRD patterns of Fig. 5 (1 h), it can be observed that all the peaks of samples for 1 h belong to V_2O_5. After 3 h, the peaks of V_2O_5 disappeared, but the

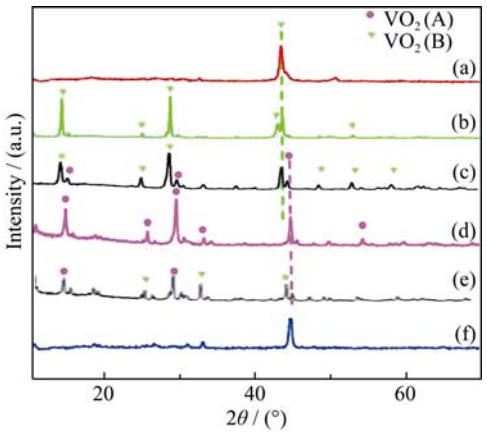

Fig. 4　XRD patterns of samples obtained at different temperatures and MR for 24 h
(a) MR is 2: 1, 180 ℃; (b) MR is 2: 1, 200 ℃; (c) MR is 2: 1, 220 ℃; (d) MR is 3: 1, 220 ℃; (e) MR is 3: 1, 200 ℃; (f) MR is 3: 1, 180℃

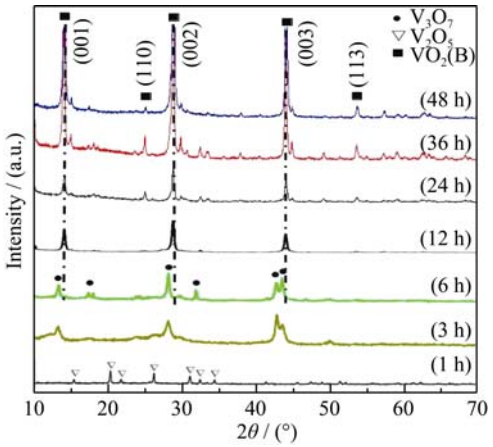

Fig. 5　XRD patterns of samples obtained after different amounts of time at 200℃ with a molar ratio of 2: 1 for reducing agent to vanadium source
(a) 1 h; (b) 3 h; (c) 6 h; (d) 12 h; (e) 24 h; (f) 36 h; (f) 48 h

peaks belonging to $V_3O_7{\cdot}H_2O$ appeared as shown in Fig. 5 (3 h) and (6 h), which reveals that the reduction reaction has started and the sample has been reduced to $V_3O_7{\cdot}H_2O$. With further increase of the time to 12 h and 24 h, all the peaks are consistent with the characteristic peaks of VO_2 (B) as shown in Fig. 5 (12 h). For the samples with a reaction time of 36 h and 48 h, the (110) and (113) peaks belonging to VO_2(B) significantly enhanced.

Thus, the optimal synthesis condition of ultra-long VO_2(B) is hydrothermal treatment of an aqueous solution of V_2O_5 and BHT at 200℃ for 24 h with a molar ratio of 2:1. Compared with other reports on VO_2(B), the preparation process is not only simple but also time saving. Moreover, the crystallinity of VO_2(B) is still very high, the phase is quite pure and the morphology is very uniform.

2.2 The electrochemical properties

Electrochemical properties of the as synthesized vanadium oxidesbased electrodes were evaluated using galvanostatic charge/discharge as shown in Fig. 6. Figure 6(a) displays the rate capability of the VO_2(B) at different rates from 50 to 2000 mA/g. The discharge capacity for the VO_2(B) nanobelts initiates at 437.0 mAh/g which is very closely to Tarascon's results who gave us an amazement crystalline VO_2(B) exhibited a specific capacity as high as 500 mAh/g[8]. The discharge capacity drastically drops to 225 mAh/g within fifth cycles, which could be attributed to the structure compacted or irreversible phase transformation of active materials during repeatedly charge/discharge process[23]. Moreover, at 100, 200, 500, 1000 and 2000 mA/g, the electrode exhibits discharge capacities of 175, 125, 90, 75 and 50 mAh/g, respectively. Even at ultrahigh current densities of 2000 mAh/g, the nanobelts can still deliver a capacity of 50 mAh/g, indicating superior rate performance. Furthermore, no capacity fading is observed at discharge rates higher than 50 mA/g. The nanobelts could tolerate a larger crystal volume change and remain more stable, and thus allowing good cycling stability at high rates.

As reported, VO_2(B) with various morphologies could hardly exhibit good cyclability. Specific capacity irreversibly fades quickly due to the electrodes side reaction and structural transformation. Though batteries with nanoscale materials deliver more power quickly with less heat, an increase in undesirable electrode/electrolyte reactions leads to self-discharge, poor cycling and calendar life[24]. It remains a great challenge to improve the cycling performance of VO_2(B) for chemists and material scientists. Figure 6(b) shows long-term cycling performance up to 500 cycles at high current density of 1000 mA/g. The nanobelts exhibit an initial discharge capacity of 141.3 mAh/g at 1000 mA/g. The discharge capacity increases with the cycle number during the initial ~323 cycles, to a maximum value of 303.2 mAh/g at the 323th cycle, which is probably due to the enhanced electrode polarization at high current density[23]. Such phenomenon suggests the inferior intrinsic kinetic diffusion ability for VO_2 in the first several insertion/extraction processes. V_2O_5 also shows the enhanced discharge capacity in present reported work[24-25]. After 323 cycles, the discharge capacity decreased to 126.6 mAh/g at 500th cycle. Charge/discharge capacity irreversibly fades due to the electrodes side reaction and structural transformation which was also shown in other literature[23]. The capacity retention is as high as 89.59% after 500 cycles, while most of earlier reports illustrated that the capacity retention is lower than 70% after 100 cycles when used VO_2(B) as cathode materials[23-24, 26-28]. Such superior cyclability better than those in the previously reported VO_2(B) cathode nanomaterials are very promising to meet the requirements for many long-term high-power applications.

The kinetic mechanism of vanadium oxides electrodes were discussed by CV technique at a scan rate of 0.2 mV/s in the voltage window from 1.5 V to 4.5 V *vs* Li^+/Li. As clearly shown in Fig. 6(c), wide flat reduction and oxidation peaks were observed, corresponding to the insertion and extraction of lithium ions, suggesting that the as-obtained ultra-long belt-like VO_2(B) nanomaterials can reversibly deliver the lithium ions during cell operation. Therefore, we think that VO_2(B) is fitter for as capacitor materials than other lithium battery which indicated a one-step lithiation/delithiation process, due to their structural changes upon the one Li^+ ion insertion/extraction process, corresponding to the following phase transition (Equation 1)[25]:

$$VO_2 + Li^+ + e^- \leftrightarrow LiVO_2 \quad (1)$$

Galvanostatic cycling tests showed us the detailed description about the variation of the specific capacity versus voltage (*vs* Li^+/Li) as indicated in Fig. 6(d). No obvious charge/discharge plateau but an asymmetrical capacitor behavior was observed, implying promising capacitive performance rather than lithium storage[29-30]. This result was corresponding to that of the CV curves (Fig. 6(c)).

Above all, the VO_2(B) nanobelts showed excellent electrochemical properties, including high discharge capacity, good rate capability and cyclic stability. These are all the reasons for which these belt-like VO_2(B) had a better cycling performance. Thus, the ultra-long VO_2(B) nanobelt is the candidate cathode materials for rechargeable SCPs.

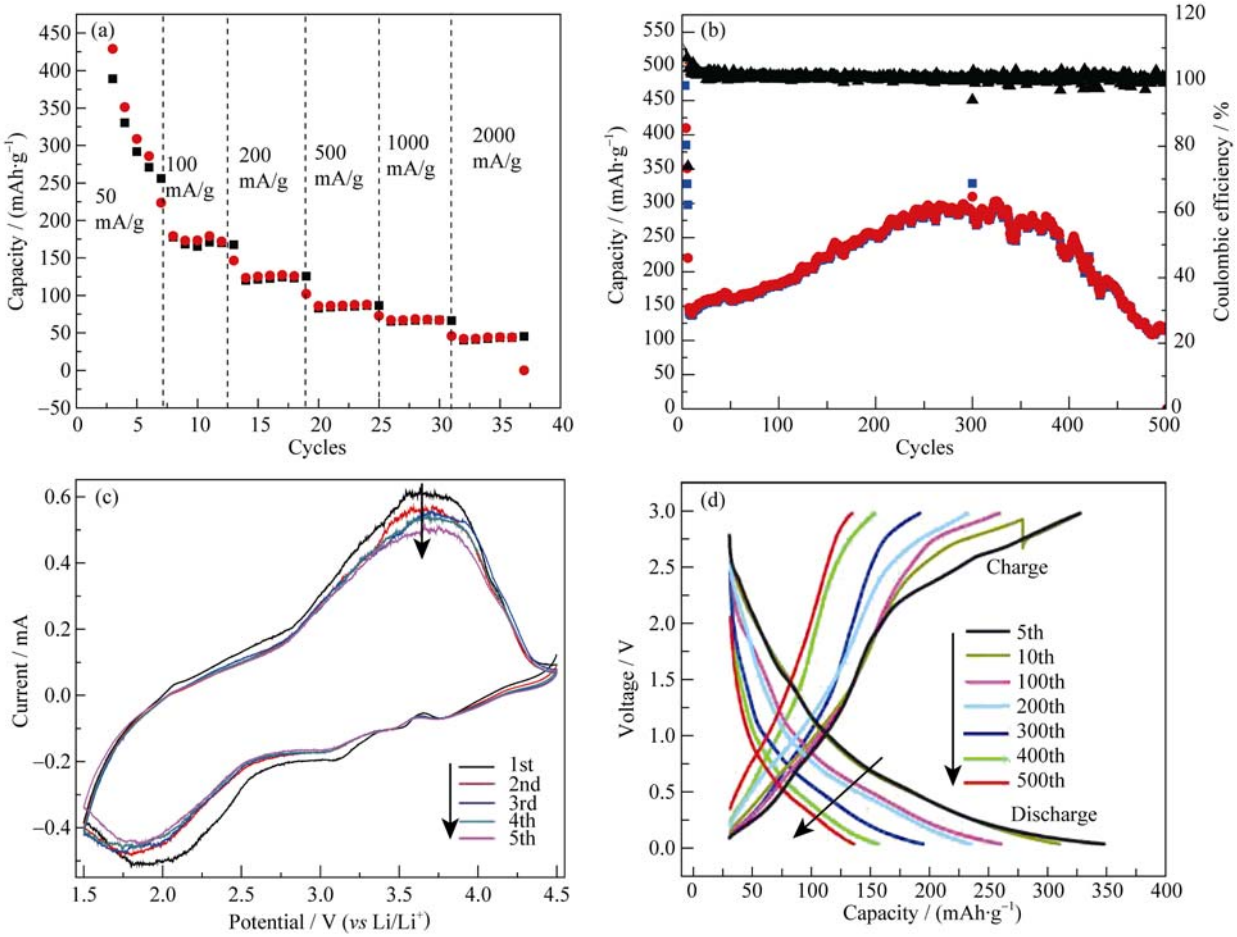

Fig. 6　Electrochemical properties of as-prepared VO_2 nanobelts

(a) Rate performance of as-prepared VO_2(B) nanobelt at various current densities from 50 mA/g up to 2000 mA/g; (b) Charge/discharge curves and coulombic efficiency *vs* cycle number of VO_2(B) nanobelt; (c) Cyclic voltammograms of VO_2(B) nanobelts obtained at a scan rate of 0.2 mV/s; (d) Voltage *vs* capacity curves of the as-prepared VO_2(B) between 0 Vand 3 V

3　Conclusions

Well-crystallized and ultra-long VO_2(B) nanobelts were directly synthesis using a facile one-step hydrothermal procedure. The achieved nanobelts were dozens of microns in length and ~200 nm in width, respectively, and the optimal synthesis condition is hydrothermal under 200 ℃ for 24 h with MR=2: 1. The VO_2(B) nanobelts exhibited an ultra-high rate performance of 425 mAh/g at 50 mA/g. Especially, excellent cycling stability with a low capacity loss of 10.41% over 500 cycles at 1000 mA/g, successfully solved the problem of poor cycling and calendar life. The fascinating electrochemical performance makes the VO_2(B) nanobelts a promising candidate as cathode materials for high power SCPs.

References:

[1] TARASCON J M, ARMAND M. Issues and challenges facing rechargeable lithium batteries. *Nature*, 2001, **41(15):** 359–367.

[2] WAN G X, SUN L, BRADHURST D H, *et al*. Nanocrystalline NiSi alloy as an anode material for lithium-ion batteries. *J. Alloys Compd.*, 2000, **306 (1/2):** 249–252.

[3] ARICO A S, BRUCE P, SCROSAIT B, *et al*. Nanostructured materials for advanced energy conversion and storage devices. *Nat. Mater.*, **2005, 4(5):** 366–377.

[4] ZHANG T, GAO J, FU L J, *et al*. Natural graphite coated by Si nanoparticles as anode materials for lithium ion batteries. *J. Mater. Chem.*, 2007, **17:** 1321–1325.

[5] PATIL U M, SALUNKHE R R, GURA K V, *et al.* Chemically deposited nanocrystalline NiO thin films for super capacitor application. *Applied Surface Science*, 2008, **255:** 2603–2607.

[6] HUANG S H, WEN Z Y, LIN B, *et al.* The high-rate performance of the newly designed $Li_4Ti_5O_{12}$/Cu composite anode for lithium ion batteries. *J. Alloys Compd.*, 2008, **457:** 400–403.

[7] WEI M, SUGIHARA H, HONMA I, *et al.* A new metastable phase of crystallized $V_2O_4{\cdot}0.25H_2O$ nanowires: synthesis and electrochemical measurements. *Adv. Mater.*, 2005, **17(24):** 2964–2969.

[8] BAUDRIN E, SUDANT G, LARCHER D, *et al.* Preparation of nanotextured VO_2[B] from vanadium oxide aerogels. *Chem. Mater.*, 2006, **18(18):** 4369–4374.

[9] ODANI A, POL S V, KOLTYPIN M, *et al.* Testing carbon-coated VO_x prepared *via* reaction under autogenic pressure at elevated temperature as Li - insertion materials. *Adv. Mater.*, 2006, **18:** 1431.

[10] ROJAS D M, BAUDRIN E. Synthesis and electroactivity of hy-

drated and monoclinic rutile-type nanosized VO_2. *Solid State Ionics*, 2007, **178(21/22):** 1268–1273.

[11] MAI L Q, XU L, HAN C H, *et al.* Electrospun ultralong hierarchical vanadium oxide nanowires with high performance for lithium ion batteries. *Nano Lett.,* 2010, **10(11):** 4750–4755.

[12] JU S H, KANG Y C. Morphological and electrochemical properties of LiV3O8 cathode powders prepared by spray pyrolysis. *Electrochim. Acta*, 2010, **55(20):** 6088–6092.

[13] SAKUNTHALA A, REDDY M V, SELVASEKARAPANDIAN S, *et al.* Energy storage studies of bare and doped vanadium pentoxide $V_{1.95}M_{0.05}O_5$(M = Nb, Ta) for lithium ion batteries. *J. Phys. Chem. C*, 2010, **114:** 8099–8107.

[14] LI H Q, HE P Y, WANG G, *et al.* High-surface vanadium oxides with large capacities for lithium-ion batteries: from hydrated aerogel to nanocrystalline VO_2(B), V_6O_{13} and V_2O_5. *J. Mater. Chem*., 2011, **21:** 10999–11009.

[15] YANG S B, GONG Y J, LIU Z, *et al.* Bottom-up approach toward single-crystalline VO_2-graphene ribbons as cathodes for ultrafast lithium storage. *Nano Lett.*, 2013, **13(4):** 1596−1601.

[16] LI H Q, ZHAI T Y, HE P, *et al.* Single-crystal $H_2V_3O_8$ nanowires: a competitive anode with large capacity for aqueous lithium-ion batteries. *J. Mater. Chem*., 2011, **21:** 1780–1787.

[17] CAO A M, HU J S, LIANG H P, *et al.* Self-assembled vanadium pentoxide (V_2O_5) hollow microspheres from nanorods and their application in lithium-ion batteries. *Angew. Chem., Int. Ed.*, 2005, **44(48):** 4391–4393.

[18] WANG Y, CAO G Z. Synthesis and enhanced intercalation properties of nanostructured vanadium oxides. *Chem. Mater.*, 2006, **18(12):** 2787–2804.

[19] ROLISON D R, DUNN B. Electrically conductive oxide aerogels: new materials in electrochemistry. *J. Mater. Chem*., 2001, **11:** 963.

[20] XU Y J, HUANG W X, SHI Q W, *et al.* Synthesis and properties of Mo and W ions co-doped porous nano-structured VO_2 films by Sol–Gel process. *J. Sol-Gel Sci. Technol.*, 2012, **64 (2):** 493–499.

[21] XU Y J, HUANG W X, SHI Q W, *et al.* Shape-dependent thermochromic phenomenon in porous nano-structured VO_2 films. *Materials Research Bulletin,* 2013, **48(10):** 4146–4149.

[22] SHI Q W, HUANG W X, ZHANG Y X, *et al.* Giant phase transition properties at terahertz range in VO_2 films deposited by Sol-Gel method. *ACS Appl. Mater. Interfaces*, 2011, **3(9):** 3523–3527.

[23] LIU Y Y, UCHAKER E, ZHOU N, *et al.* Facile synthesis of nanostructured vanadium oxide as cathode materials for efficient Li-ion batteries. *J. Mater. Chem.*, 2012, **22:** 24439–24445.

[24] HUANG J J, WANG X F, LIU J F, *et al,* Flexible free-standing VO_2(B) nanobelt films as additive-free cathode for lithium-ion batteries. *J. Power Sources*, 2013, **222:** 21–31.

[25] ZHAO H B, PAN L Y, XING S Y. Vanadium oxidese-reduced graphene oxide composite for lithium-ion batteries and supercapacitors with improved electrochemical performance. *J. Power Sources*, 2013, **222:** 21–31.

[26] MAI LIQIANG. Vanadium oxide nanowires for Li-ion batteries. *J. Mater. Res.*, 2011, **26(17):** 2175–2185.

[27] NETHRAVATHI C, RAJAMATHI C R, RAJAMATHI M. N-doped graphene-VO_2(B) nanosheet-built 3D flower hybrid for lithium ion battery. *ACS Appl. Mater. Interfaces*, 2013, **5:** 2708−2714.

[28] LI N, HUANG W X, SHI Q W. A CTAB-assisted hydrothermal synthesis of VO_2(B) nanostructures for lithium-ion battery application. *Ceramics International*, 2013, **39:** 6199–6206.

[29] MAI L Q, WEI Q L, AN Q Y, *et al,* Nanoscroll buffered hybrid nanostructural VO_2(B) cathodes for high-rate and long-life lithium storage. *Adv. Mater.,* 2013, **25:** 2969–2973.

[30] ZHANG S D, LI Y M, WU C Z, *et al,* Novel flowerlike metastable vanadium dioxide (B) micronanostructures: facile synthesis and application in aqueous lithium ion batteries. *J. Phys. Chem. C*, 2009, **113:** 15058–15067.

一步水热法制备超长 VO_2(B)纳米带及其电化学性能

杨雪梅[1,2], 刘忠平[1,2], 李小东[1,2], 张泽明[2], 纪兰香[2], 邓建国[1,2]

(1. 中国工程物理研究院 化工材料研究所, 绵阳 621900; 2. 四川省新材料中心, 绵阳 621000)

摘 要: 采用简易的一步水热法制备了超长的 VO_2(B)纳米带。对纳米带的结构、形貌、最优合成条件及电化学性能进行了研究。结果发现: 制得的 VO_2(B)纳米带长度约为几十微米, 宽度为~200 nm; 且最优合成条件为在钒源与还原剂摩尔比为 2:1 的条件下, 200℃水热反应 24 h。当该 VO_2(B)纳米带被作为锂离子电池的阳极材料时, 显示出了优异的电化学性能, 尤其是循环稳定性, 循环 500 周后的电容量损失率仅为 10.41%, 极大的解决了钒类纳米材料作为锂离子电池阳极材料时稳定性差的问题, 提高了其成为锂离子电池阳极材料的可能性。

关 键 词: VO_2(B); 纳米带; 电化学性能

中图分类号: TM912 **文献标识码:** A